AD-A142 303 HIGH CURRENT INDUCTION ACCELERATORS(U) NAVAL RESEARCH LAB WSSHINGTON DC C A KAPETANAKOS ET AL. 12 JUN 84 NRL-MR-5259 1/1

UNCLASSIFIED F/G 20/7 NL

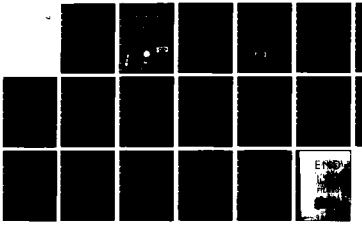

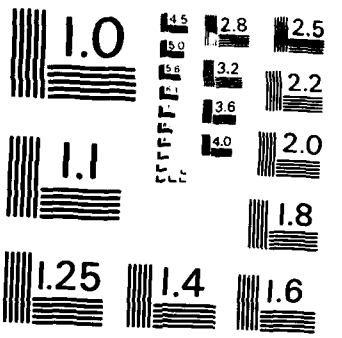

(2)

NRL Memorandum Report 5259

High Current Induction Accelerators

C. A. KAPETANAKOS

Beam Dynamics Program
Plasma Physics Division

P. SPRANGLE

Plasma Theory Branch
Plasma Physics Division

06 21 185

AD-A142 302

REPORT DOCUMENTATION PAGE

1a REPORT SECURITY CLASSIFICATION UNCLASSIFIED	1b RESTRICTIVE MARKINGS
2a SECURITY CLASSIFICATION AUTHORITY	3 DISTRIBUTION AVAILABILITY OF REPORT Approved for public release; distribution unlimited.
2b DECLASSIFICATION DOWNGRADING SCHEDULE	
4 PERFORMING ORGANIZATION REPORT NUMBER S NRL Memorandum Report 5259	5 MONITORING ORGANIZATION REPORT NUMBER S
6a NAME OF PERFORMING ORGANIZATION Naval Research Laboratory	6b OFFICE SYMBOL (If applicable) Code 4704
7a NAME OF MONITORING ORGANIZATION Office of Naval Research	
6c ADDRESS (City, State and ZIP Code) Washington, DC 20375	7b ADDRESS (City, State and ZIP Code) Arlington, VA 22217
8a NAME OF FUNDING SPONSORING ORGANIZATION	8b OFFICE SYMBOL (If applicable)
9 PROCUREMENT INSTRUMENT IDENTIFICATION NUMBER	
8c ADDRESS (City, State and ZIP Code)	10 SOURCE OF FUNDING NOS

PROGRAM ELEMENT NO	PROJECT NO	TASK NO	WORK UNIT NO
61153N		RR011-09-4E	DN180-207

11 TITLE (Include Security Classification) High Current Induction Accelerators	
12 PERSONAL AUTHOR(S) C.A. Kapetanakos and P.A. Sprangle	
13a TYPE OF REPORT Interim	13b TIME COVERED FROM TO
14 DATE OF REPORT (Yr., Mo., Day) June 12, 1984	15 PAGE COUNT 32
16 SUPPLEMENTARY NOTATION	

17 COSATI CODES			18 SUBJECT TERMS (Continue on reverse if necessary and identify by block number)
FIELD	GROUP	SUB GR	Accelerators Induction accelerators Electron beams

19 ABSTRACT (Continue on reverse if necessary and identify by block number)

High energy accelerators capable of producing high current electron beams are rapidly becoming an active area of research. The main development effort is currently being focused on induction accelerators. As a result of their inherent low impedance, these devices are ideally suited for generating intense beams. If this high current branch of accelerator technology is successful, it may have some very profound implications, far beyond the research laboratories.

20 DISTRIBUTION AVAILABILITY OF ABSTRACT UNCLASSIFIED UNLIMITED X SAME AS RPT DTIC USERS	21 ABSTRACT SECURITY CLASSIFICATION UNCLASSIFIED
22a NAME OF RESPONSIBLE INDIVIDUAL C.A. Kapetanakos	22b TELEPHONE NUMBER (Include Area Code) (202) 767-2838
	22c OFFICE SYMBOL Code 4704

DD FORM 1473, 83 APR EDITION OF 1 JAN 73 IS OBSOLETE

CONTENTS

HIGH CURRENT INDUCTION ACCELERATORS

I. Introduction

In order to probe deeper into the sub-nuclear structure of matter, physicists over the last fifty years have advanced the technology of high energy accelerators to a remarkable level of sophistication. These accelerators have been designed to operate at relatively low current levels primarily to avoid complications related to beam self field effects. Accelerators such as the SLAC Linear Accelerator at Stanford University currently produces electron beams with energies as high as 32 GeV and peak currents of approximately 120 mA. Although of fairly low current, these devices have proven extremely successful in high energy physics applications, since by irradiating the target over an extended period of time a detectable level of collisional events could be obtained.

In addition to low current high energy accelerators, a new technology for producing ultra-high current beams[1-3] has sprung out of x-ray flash research in the early 1960s. Unfortunately, the new technology was limited to peak beam energies below 15 MeV. These ultra-high current beams typically last for a fraction of a microsecond and have peak currents as high as 10 MA. Such beams contain enough energy to melt holes in millimeter thick aluminum targets and have self field energies comparable to the beam kinetic energy.

Over the last several years, it has become apparent that electron beams having both high energy and high current could have exciting applications in the generation of high power coherent radiation[4], x-ray radiography and national defense[5].

Among the various accelerating schemes that have the potential to produce ultra-high power electron beams, induction accelerators appear to be the most promising. Induction accelerators are inherently low impedance devices and

Manuscript approved March 8, 1984.

thus are ideally suited to drive high current beams. The acceleration process is based on the inductive electric field produced by a time varying magnetic field. The electric field can be either continuous or localized along the acceleration path.

The current level of sophistication of induction accelerators is considerably lower than that of conventional low-current accelerators. This is not surprising since the fiscal and human resources invested in conventional accelerators far exceeds those invested in developing high current induction accelerators.

Quite naturally, induction accelerators are divided into linear and cyclic. The linear devices are in turn divided into Astron-type[6-10], Radlac-type[11-12] and auto-accelerator[13-14]. In the first type, ferromagnetic induction cores are used to generate the accelerating field, while "air core" cavities are used in the second. In the auto-accelerator the air core cavities are excited by the beam's self fields rather than external fields. Similarly, cyclic devices can be divided into conventional[15,17] and modified betatrons[18-21]. The field configuration in the modified betatron includes, in addition to the time varying betatron magnetic field, which is responsible for the acceleration, a strong toroidal magnetic field that substantially improves the stability of the accelerated beam.

Linear accelerators are currently in a more advanced state of development than their cyclic counterpart, however, their size and high cost make them unattractive when high energies are desired. For this reason, progressively more attention is being focused on cyclic induction accelerators. Table I lists the known high current induction accelerators throughout the world.

Table I

High-Electron Current Induction Accelerators

Device	Laboratory (Country)	Type	Year	Energy (MeV)	Current (kA)	Duration (nsec)	Rep. Rate (Hz)	Comments
Astron	LLL(USA)	ASTRON	1963 1968	4 6	0.2 0.8	300 300	60 5	Disassembled Disassembled
FXR	LLL(USA)	ASTRON	1979	20	4	40	-	-
ERA-inj	Berkeley(USA)	ASTRON	1971	4	0.9	2-45	1-5	Disassembled
NEP-2,inj	Dubna(USSR)	ASTRON	1971	30	0.25	500	50	-
NBS	NRL(USA)	ASTRON	1973	0.8	1	2,000	SP	Long Pulse
ETA	LLL(USA)	ASTRON	1979	4	8	30	1	In Operation
ATA	LLL(USA)	ASTRON	1984	<50>	<10>	<50>	<1-10>	Under Testing
LIU-10	(USSR)	RADLAC	1977	13.5	50	20 or 40	-	-
Radlac-I	SNL(USA)	RADLAC	1980	9	25	12	SP	Disassembled
IBEX	SNL(USA)	RADLAC	1982	4	30	20	SP	In Operation
Radlac II	SNL(USA)	RADLAC						
Auto-Accel.	(USSR)	AUTO	1974	1.0	5-15	-	SP	-
Auto-Accel.	NRL(USA)	AUTO	1962	7.3	70	10	SP	-
Betatron	(USSR)	CYCLIC	1964	100	0.1	-	SP	-
Mod. Betatron	Irvine(USA)	CYCLIC	1983	<10>	<1>	-	SP	Under Testing
Mod. Betatron	NRL(USA)	CYCLIC	1986	<50>	<5-10>	-	SP	Under Constr.

< > indicates design value; SP = single pulse

II. Linear Induction Accelerators (LIA)

As stated in the introduction, linear induction accelerators are divided into two types. The Astron-type was pioneered by N. Christophilos at Lawrence Livermore National Laboratory (LLNL) in 1963 and the Radlac type was pioneered by Pavlovskii and coworkers in the Soviet Union.

a. Astron-type

To illustrate the underlining physical mechanism of a single accelerating module, consider a coil wound around a ferromagnetic ring powered by a time varying voltage source as shown in Fig. (1). The voltage V_g across the opening (gap) of a single turn loop surrounding the ferromagnetic core can be found by integrating Faraday's law along the loop and is given by

$$V_g = - \int \vec{E} \cdot d\vec{\ell} = \frac{1}{c} \frac{\partial}{\partial t} \cdot \qquad (1)$$

The voltage V_g is proportional to the time rate of the magnetic flux ϕ linking the loop, where $\phi = \int \vec{B} \cdot d\vec{S}$ is the integral of the magnetic field $\vec{B}$ over the area enclosed by the loop.

An Astron-type LIA consists of several induction modules placed in tandem and synchronized to provide an accelerating field when the beam passes the gap. Figure 2 shows a two module LIA utilizing Blumleins to drive the ferromagnetic core, although other power supplies, such as modulators, are frequently used.

In a Blumlein, a load is located midway between the ends of the transmission line. At t = o the switch, which is located at the beginning of the line, is closed, initiating a voltage step which propagates along the first half of the folded line until it reaches the load. Under matched conditions the load has an impedance equal to twice the characteristic

impedance Z_o of the line. Upon arriving at the load, the voltage pulse is partially reflected toward the switch and the remaining part is transmitted to the other half of the line. When the Blumlein is initially charged to the voltage V_o and the load impedance is 2 Z_o, the voltage across the load becomes equal to V_o. The reflected voltage pulse propagates toward the short (switch) and is reflected with opposite polarity. The transmitted pulse reaches the open end of the line and is reflected with the same polarity. The two reflected pulses completely discharge the line as they travel toward the load. Consequently, the voltage across the load is a rectangular pulse of amplitude V_o and duration $2\,\ell/u = 2\tau$, where ℓ is the length of the line and u is the pulse propagation speed.

The voltage appearing across the load drives the coil that magnetizes the ferromagnetic core. Since the coil inductance L is large, i.e., $\pi L/\tau \gg Z_o$, the current flowing through the coil is considerably smaller than that in the Blumlein. Therefore, the effect of the magnetizing coil on the operation of the Blumlein can be ignored.

The energy gained by an electron propagating along the dashed line in Fig. 2 can be found by integrating the energy rate equation

$$\Delta W = -|e| \int \vec{E} \cdot d\vec{\ell} = \frac{|e|}{c} \frac{\partial \Phi}{\partial t} = 2|e|\, V_g \approx 2|e|\, V_o, \qquad (2)$$

provided the two modules are identical and the Blumleins are initially charged to the same voltage V_o. In induction accelerators the energy gain per module is additive so that for N modules the electron energy gain is $N\,|e|\,V_o$. In contrast, in a similar electrostatic accelerator the electron would gain only an energy $|e|\,V_o$.

The pulse duration in the Astron-type LIA varies from 20 nsec to a few microseconds. For pulses of 100 nsec or shorter the core is made of ferrite. For longer pulses the core is made of thin sheets of less expensive laminated ferromagnetic materials. The size of the core is mainly determined by the limiting current and image forces. The length of the accelerator is set by the maximum electron energy desired while the cross section of the core is determined by the product $V_g \tau_s$, where τ_s is the core saturation time.

Some of the distructive instabilities limiting the performance of Astron-type LIA are; beam breakup, image displacement and resistive wall instabilities. The beam breakup instability appears to be the most serious and arises from the interaction of the beam with resonant modes of the accelerating cavities. These modes have a strong magnetic field component, at the beam position, perpendicular to the direction of propagation. In each cavity the beam experiences a transverse displacement, which increases exponentially with the number of cavities and beam current. The beam breakup instability has been observed in several accelerators including the Astron, ETA and ATA.

The size and cost of these accelerators may become prohibitive at high energies. Currently, the maximum average accelerating gradient is less than 1 MV/m. Therefore, a 1 GeV acceleration would be longer than 1 km and require in excess of 4,000 accelerating modules and several thousand quadrupole focusing lenses. It is conceivable that advances in technology will improve the accelerating gradient by a factor of three or so with a corresponding reduction in length, and perhaps cost.

Two recent advances in technology may have a significant impact on LIA development. The first is the development by Lawrence Livermore National Laboratory of magnetic switches capable of repetition rates in excess of 10 KHz. These switches are based on high power saturable reactors, which have a

high inductance during charging, that is rapidly reduced when the core saturates. The second advance is related to the development of Metglass, a high resistivity ferromagnetic tape, that has a saturation flux density 3 to 5 times higher than ferrite. Consequently cores made of Metglass will have a cross section 3 to 5 smaller than ferrite cores.

To date eight high current Astron-type LIA have been developed and their salient parameters are listed in Table I. The most advanced among these is the Advanced Test Accelerator (ATA) presently under testing at LLNL. As of November 1983 the ATA has produced a 2 kA, 40-50 MeV electron beam.

b. Radlac-type

As with all induction accelerators, the accelerating field in the Radlac is due to the rate of change of magnetic flux. The basic accelerating process can be understood by considering a single accelerating module as shown in Fig. 3a. The module is a folded transmission line capable of supporting a propagating electromagnetic wave. Initially, i.e., prior to beam injection, the central conductor of the module is charged to a voltage V_o with respect to the outer conductors. At time $t = o$ the beam is injected and the switch connecting points a and b is closed. The short initiates a traveling voltage pulse which propagates toward the open gap (points b and c). The electric field across the gap remains constant for a transit time $\tau = \ell/u$. If the transmission line is not loaded with dielectric material the pulse velocity is approximately equal to the speed of light, $u \approx c$. The propagating pulse arrives at the gap at time τ, with its electric field directed opposite to the initially imposed field. The field is reflected at the open gap without changing polarization. The net electric field (sum of the initial, incident and reflected) across the gap reverses direction at time τ and remains constant for a time interval equal to 2τ. The electric field pulse changes

direction upon reflection at the shorted end (switch) and arrives back at the gap at time 3τ resulting in a reversal of the net electric field across the gap. The field across the gap is thus (see Fig. 3b) an alternating series of rectangular pulses each of duration 2τ, except the first pulse which lasts for a time τ.

As in the Astron-type LIA, the change in particle energy in traversing the gap, ΔW, is proportional to the line integral of the electric field across the gap, which in turn is proportional to the rate of change of magnetic flux. Electrons traversing the gap will gain an energy equal to the initi voltage of the transmission line, i.e., $\Delta W = |e| V_o$. Prior to closing tl switch the electric field across the gap is conservative (electrostatic) t becomes inductive immediately following switch closure. Hence for N modu ., each initially charged to voltage V_o, the net particle energy gain will be $|e|$ NV_o, provided that the switches are properly synchronized. The electron pulse length must necessarily be less than τ if the first pulse is used and less than 2τ for subsequent pulses.

Pavlovskii and coworkers in 1977 reported the generation of a 13.5 MeV, 50 kA electron beam. Figure 4 shows the Radlac I accelerator constructed at Sandia Laboratories. This device, based on Pavlovskii's design, uses four radial lines filled with oil and eight self-breaking spark-gap switches. The radially tapererd cavities provide constant impedance along the entire length of the line. Radlac II, currently under construction at Sandia Laboratories uses water filled strip lines and has been designed to generate higher power pulses than Radlac I.

The main advantages of the Radlac concept are high accelerating gradients and high efficiency. The main limitations are formation of virtual cathodes at the gaps, poor beam quality and poor beam stability characteristics.

Average accelerating gradients of approximately 3 MV/m have been demonstrated in both the Soviet LIU and Radlac I. To achieve higher accelerating gradients, the vacuum insulator interface must be stressed far above the flashover electric fields obtained with alternating polarity pulses. This may be accomplished by designing the transmission lines to produce single polarity voltage pulses.

The efficiency of radial line accelerators can be very high. For example, the calculated efficiency of a 100 kA accelerator, with an average gradient of 3 MV/m, is approximately 75% but drops as the accelerating gradient increases.

The beam quality in Radlac I was considerably less than desired. Both the current and voltage wave forms were triangular and although the emittance has not been measured, it is probably quite high. It appears that a substantial amount of work is needed to improve the beam quality.

The most disruptive instabilities limiting the performance of the Radlac are the diocotron, beam breakup, image displacement and resistive wall. As in the Astron-type accelerators, probably the most serious instability for a 1 GeV, 100 kA device is the beam breakup mode, which has a growth rate proportional to the beam current and number of accelerating gaps.

c. Auto-accelerator

In the previously described devices, the accelerating inductive electric field is produced by a time varying external magnetic field. In the auto-accelerator[13,14] the electric field responsible for the acceleration is generated by the interaction of the beam with a cavity structure. Briefly, a segment of the beam stores electromagnetic energy in a cavity at the expense of its kinetic energy. The stored energy is subsequently transferred to the

remaining section of the beam, resulting in a shorter duration beam of higher energy.

The auto-accelerator is shown schematically in Fig. 5a. The voltage appearing across the gap is again given by Eq. (1). The sudden appearance of the voltage across the gap results in the excitation of cavity modes. For a constant current beam (Fig. 5b) the radial electric field and the azimuthal magnetic field within the cavity are given by $B_\varphi = (u/c)E_r = -2|I_b|/cr$. For a pure TEM mode traveling with velocity u, the flux within the cavity for times less than τ is $\phi = \frac{-2|I|_b}{c}$ ut $\ell n(R_2/R_1)$, where R_1 is the inner and R_2 the outer radii of the cavity, and I_b is the beam current. Substituting this expression for the flux ϕ into Eq. (1), we obtain the gap voltage

$$V_g = \frac{2|I_b|}{u} \ell n(R_2/R_1) = |I_b|Z_o,$$

where Z_o is the characteristic impedance of the cavity.

The electromagnetic wave travels to the shorted end of the cavity and at time τ is reflected. Upon reflection, the polorization of the electric field is reversed while that of the magnetic field remains the same. As the wave propagates from right to left the total electric field inside the cavity is progressively eliminated, while the magnetic flux increases until time 2τ. The wave arrives at the open end of the cavity at time 2τ and is again reflected with the polarization of the electric field remaining the same and that of the magnetic field reversed. After reflection from the open end the magnetic flux within the cavity starts to decrease causing the electric field at the gap to change polarity. At time 3τ the wave is reflected again from the shorted end of the line. As the electromagnetic wave propagates toward the gap both the total electric and magnetic fields in the cavity vanish. The

electric field at the gap is shown in Fig. 5c. If the duration of the beam pulse is 4τ, the leading half of the beam will be decelerated and the trailing half accelerated, resulting in a shorter beam with roughly twice the initial energy. However, when the injected beam is considerably longer than 4τ, the resulting electron pulse becomes modulated with period 4τ.

Over the last several years, the auto-accelerator concept has been investigated at the Lebedev Institute, LLNL and the Naval Research Laboratory (NRL). In a recent experiment at NRL by M. Friedman[14], a 70 kA, 4.2 MeV electron beam was auto-accelerated to 7.4 MeV without significant loss of beam current. These results were obtained with a cavity impedance of 45 Ω and a guiding magnetic field of 15 kG.

III. Cyclic Induction Accelerators (CIA)

The most striking advantage of cyclic devices, over their linear counterparts, is their compact size. Initial estimates indicate that the size advantage of cyclic accelerators is at least 1/10 that of Radlacs and approximately 1/100 that of Astron-type linear accelerators.

In cyclic induction accelerators the acceleration process is continuous. This is in contrast to LIAs in which the acceleration is localized in the gaps. Both cyclic and linear devices require the same total magnetic flux change to achieve a given energy increment. However, in the LIA the total change of flux occurs in one transit time ($\lesssim$ 100 nsec), while in the CIA the same change occurs over several thousand revolutions ($\sim$ 1 msec). As a result the peak power requirements in the CIA is approximately four orders of magnitude lower than in LIAs. Furthermore, the accelerating voltage in the CIA is about four orders of magnitude lower than in the LIA, thus reducing the complications related to high voltage insulator breakdown. Since, however,

the acceleration time is substantially longer in CIAs, collective and field nonuniformity instabilities are a far more serious problem.

The limitations on cyclic devices imposed by synchrotron radiation appear rather lenient for energies below 1 GeV. There are two pertinent issues related to synchrotron radiation: energy loss per revolution and wall survivability. The radiation energy loss per turn per electron is

$$\delta E\ [\mathrm{KeV}] = 88.5\ E^4\ [\mathrm{GeV}]/r_o[\mathrm{m}],$$

where E is the particle energy and r_o is the major radius of the particle orbit. As an illustration, for r_o = 10 m and E = 1 GeV, the radiation energy loss is 8.85 keV/turn. If the acceleration occurs within 1 msec, the energy gain per turn is about 200 keV and thus the radiative energy loss is less than 5% at peak energy.

Wall survivability due to radiation heating also does not appear to be a critical issue. The total incoherent synchrotron power radiated by an electron ring of current I is

$$P[\mathrm{Watt}] = 6\times10^{-6}\ \frac{I[\mathrm{kA}]\gamma^4}{r_o[\mathrm{m}]}.$$

For $\gamma = 2\times10^3$, I = 10 kA and r_o = 10 m, the radiative power is P = 96 MW. Since, synchrotron radiation is emitted tangentially in a cone of angle $1/\gamma$, the radiation will strike the chamber wall in a band having a width equal to the electron ring minor diameter. For example, when the beam energy rises linearly in time over 1 msec and the final minor beam radius is 1/4 cm, the peak power flux striking the wall is about $30\ \frac{KW}{cm^2}$. The estimated temperature rise at the center of the band, at normal incidence, is $\sim 100^0$C for an

aluminum chamber. However, a substantial faction of this radiation will be reflected since it strikes the chamber wall at a grazing angle and thus the temperature rise will be substantially less than 100°C.

Currently, there are two cyclic accelerators that have been studied extensively, the conventional and the modified betatron. These two devices are briefly outlined below. A variation of the modified betatron, the stellatron[22], is still in a very preliminary state of development and thus is not extensively addressed in this article.

a. Conventional Betatron

The conventional betatron is shown schematically, in Fig. 6. The toroidal accelerating electric field is generated by a time varying vertical magnetic field. During acceleration the major radius of the electrons remains constant provided the flux rule is satisified, i.e.,

$$\frac{\partial}{\partial t} \langle B_z \rangle = 2 \frac{\partial}{\partial t} B_{zo},$$

where $\langle B_z \rangle$ is the average magnetic field within the beam orbit and B_{zo} is the local field at the orbit.

To achieve both axial and radial confinement in a conventional betatron it is necessary that the external field index $n = \frac{r}{B} \frac{\partial B_z}{\partial r}$ to be between zero and unity. Magnetic configurations having such a field index can be easily obtained by suitably shaping the pole faces of the ferromagnetic core. The desired field index can also be obtained with air-core coils, although in a less straightforward way. In addition to field shaping, the ferromagnetic core minimizes the energy required to produce the magnetic field but substantially increases the weight of the device.

Space charge orbital stability in a conventional betatron requires that

the beam current satisfied the inequality

$$I_{cb}\ [kA] \leq 4.2\ (r_b/r_o)^2\ \gamma^3\ \beta^3, \qquad (3)$$

where r_o is the major electron ring radius, r_b is the minor ring radius, γ is the usual relativistic mass factor and $\beta = v/c$.

Since in any practical device the ratio (r_b/r_o) is usually less than 1/30, high currents can be confined only by increasing the injection energy, i.e., γ. For $r_b/r_o = 1/30$, the required γ to achieve 10 kA is approximately 13, i.e., an injection energy of 6 MeV.

The actual current limitation in betatrons come from instabilities such as the negative mass mode. It has been shown that the negative mass limits the electron current in a betatron below a critical current that is given approximately by the expression

$$I(kA) = [17\ \gamma\ s\ Z_o/|Z_\parallel|]\ \left(\frac{\Delta E}{E}\right)^2. \qquad (4)$$

In Eq. (4), s is the toroidal mode wavenumber, $Z_o = 4\pi/c$ is the vacuum impedance, $Z_\parallel$ is the total effective longitudinal impedance characterizing the beam environment and $\Delta E/E$ is the fractional longitudinal beam energy spread. For the parameters listed in Table II, a fractional energy spread of 4.5% results in a limiting beam current of approximately 400 A. For the same parameters Eq. (3) gives a limiting current of 28 kA.

Other less important instabilities are the transverse resistive wall, longitudinal resistive wall, ion resonance and ion streaming instability. The latter two instabilities can be excited only if a plasma is present in the chamber.

Table II
Betatron Parameters

Major electron ring radius r_o	100 cm
Minor electron ring radius r_b	5.5 cm
Electron ring injection energy E	2.5 MeV
Minor chamber radius a	16.5 cm

In addition to instabilities, other areas of concern in a conventional betatron are: i) the beam orbit displacement which is related to energy mismatch, ii) the diffusion of the self magnetic field out of the vacuum chamber and, iii) the inability of the betatron to accomodate electron rings with large transverse emittance and parallel energy spread[15].

There is extensive experience with betatrons, although such experience is almost exclusively limited to low current devices. Since the initial operation of the first device more than forty years ago, at least two hundred commercial machines have been built for industrial and medical use. The only reported high current conventional betatron was that of Pavlovskii[16] and coworkers in the USSR. They achieved a circulating beam current in excess of 100 A by injecting a 2 MeV beam into a 23 cm major radius chamber.

b. Modified Betatron

The stability properties of the conventional betatron can be substantially improved by adding a strong toroidal magnetic field[23-25]. In contrast to the betatron magnetic field, which affects mainly the major radius of the ring, the toroidal magnetic field affects primarily the minor radius. The force responsible for controlling the minor beam radius is proportional to $J_\phi B_\theta$, where J_ϕ is the poloidal ring current and B_θ is the toroidal magnetic field. As a result of this force the modified betatron can confine rings with very large emittance, i.e., large transverse velocities.

The modified betatron configuration is shown schematically in Fig. 7. In the absence of surrounding walls, space charge orbital stability requires that the electron current I_{mb} satisfy the condition

$$I_{mb}[kA] < 2.1(r_b/r_o)^2 \gamma^3 \beta^3 (B_\theta/B_z)^2.$$

Since the ratio B_θ/B_z is much greater than unity, the space charge limiting current in a modified betatron can be substantial, even for moderate values of beam energy.

In the presence of resistive chamber walls the electron current is limited by the drag instability[24]. To avoid the drag instability the beam current must satisfy the inequality

$$I_{mb}[kA] \leq 4.2\ \beta^2\ \gamma^3\ a^2/r_o^2\ , \qquad (5)$$

where a is the chamber minor radius. Note that this limiting current is independent of the toroidal magnetic field and cannot be circumvented by introducing an energy spread in the beam. In general, however, the most stringent limitation on the beam current appears to be imposed by the negative mass instability[23]. Nevertheless, even for modest values of B_θ/B_z the maximum current is substantially greater than in a conventional betatron. For example, limiting current due to the negative mass instability, with $B_\theta/B_z = 20$ and the parameters of Table II, is in excess of 5 kA. This is roughly an order of magnitude greater than in a conventional betatron.

Other less important instabilities are the resistive wall, orbital resonance, ion resonance and streaming instabilities. It has been shown, however, that a large toroidal magnetic field together with a moderate beam energy spread will have a strong stabilizing affect on these instabilities[25]. In contrast to a conventional betatron, the electron ring in a modified betatron can tolerate a substantial energy spread without significant expansion of its minor radius.

As in conventional betatrons, the beam orbit displacement resulting from an energy mismatch and the diffusion of the self magnetic field are areas of

concern. In addition, the expansion of the minor beam radius due to the crossing of single particle instability regions may be a problem area for beams with finite energy spreads.

The beam orbit displacement resulting from an energy mismatch can be substantially reduced by superimposing a stellarator[22] field on the modified betatron fields. However, this additional field, which makes the beam orbit insensitive to the energy mismatch, also makes beam trapping far more difficult. Furthermore, the electron beam may be more susceptible to orbital resonance instabilities, since the number of natural frequencies is increased with the additional stellarator field.

Presently, there are two experiments, one in the University of California at Irvine and the other at NRL, that are aimed to assess the viability of the modified betatron as a high current accelerator. The NRL experiment is scheduled to be in operation in 1984 and has been designed to produce, in full operation, a 5-10 kA, 50 MeV electron beam pulse.

IV. Comments

The development of high current accelerators would undoubtedly present some unparallel challenges to their designers. For example, consider the resulting damage to the structure, coils, septum or other components of the accelerator, in the event beam control is lost. Even if 1% of a 10 MJ beam inadvertently strikes a 10 cm^2 area, the incident energy flux is 10 kJ/cm^2. The thermal shock pressure within the material has been estimated to be approximately 500 KPSI, well above the tensile strength of copper. In addition to the damage on the various components of the accelerator, the electron beam would produce a very large, hard bremsstrahlung flux, which will require extensive radiation shielding. For the present example, the

bremsstrahlung power will be approximately 4×10^{11} watts.

It is conceivable that research on high current induction accelerators will rapidly accelerate within the next few years, provided the results from the ATA, Radlac II and the modified betatron experiments are promising. If successful, the emerging high current accelerator technology could have applications with profound implications. However, their ultimate and perhaps most important areas of application may still be unidentified.

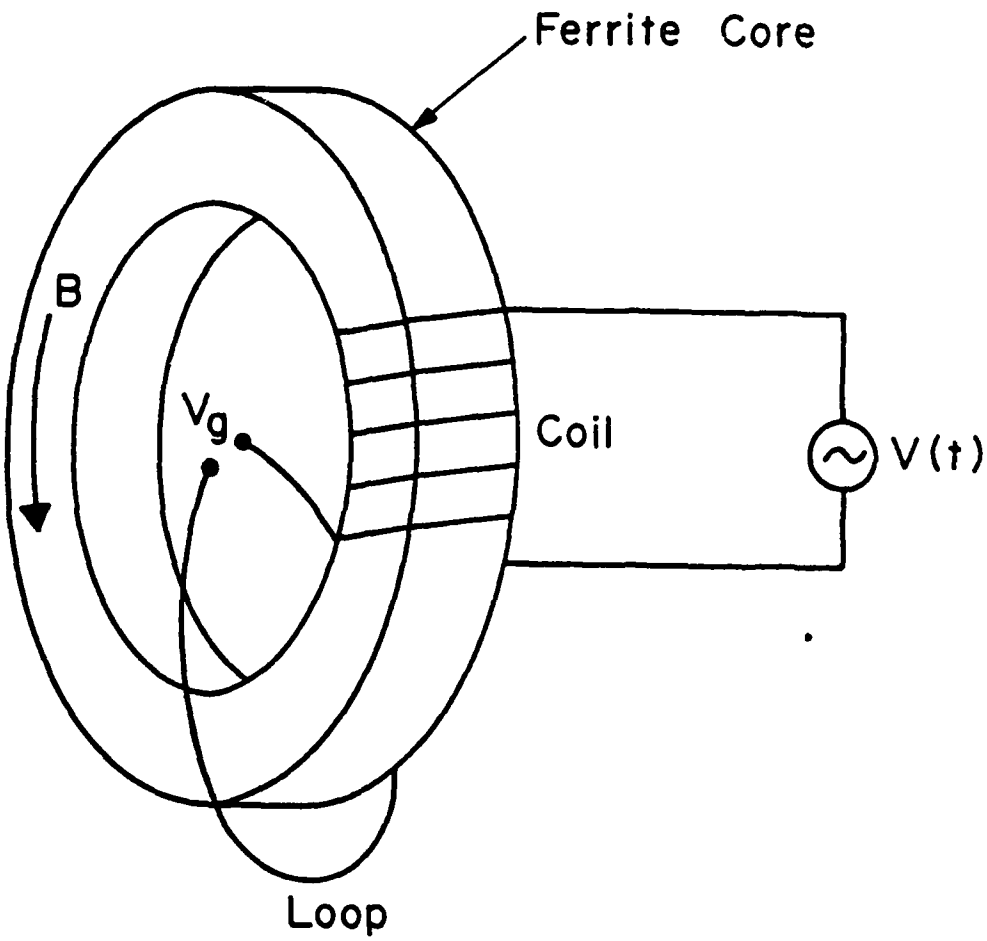

Fig. 1 Schematic of an Astron-type induction module.

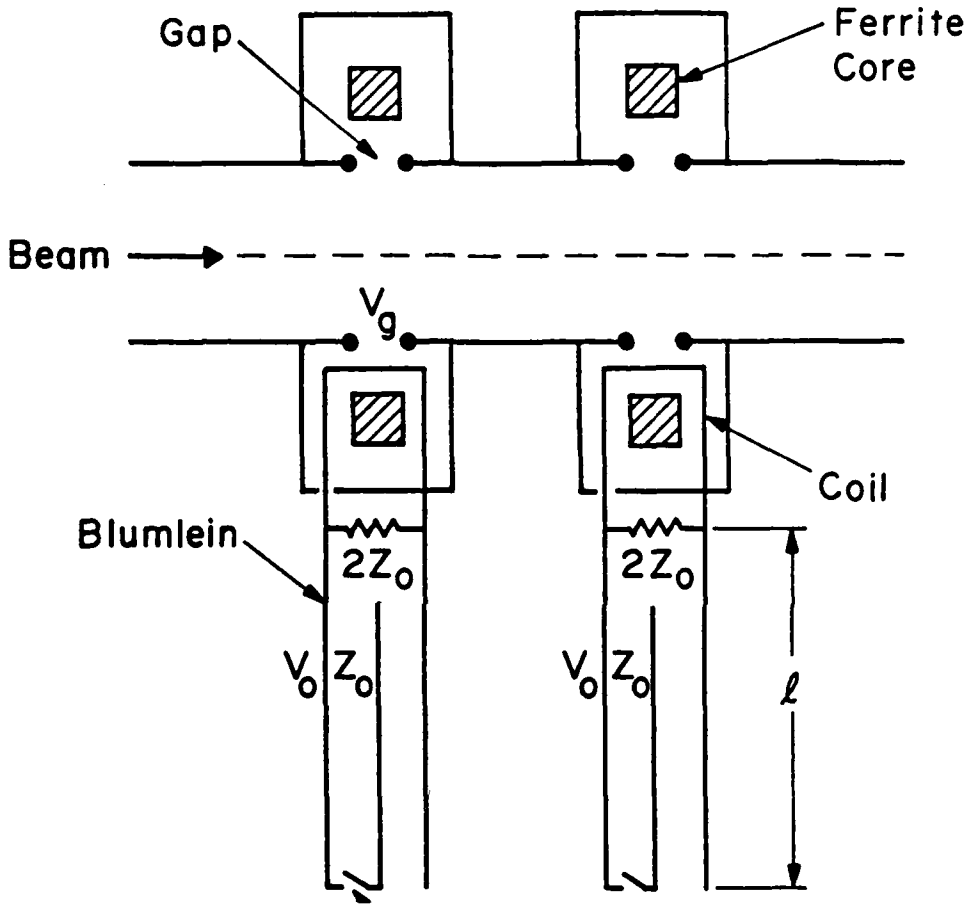

Fig. 2 Two Astron-type induction modules powered by Blumlein transmission lines.

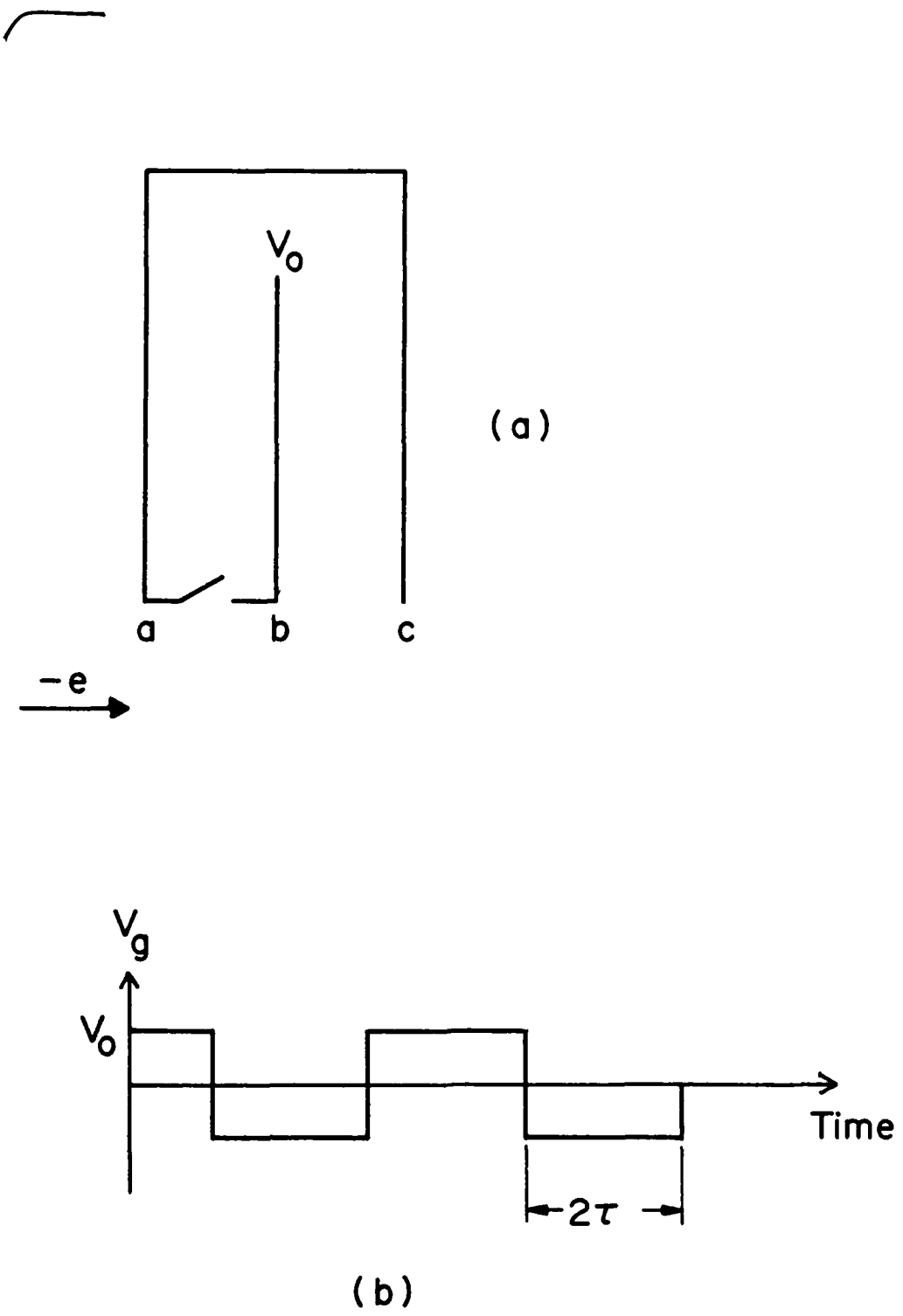

Fig. 3 (a) Schematic of a Radlac-type induction module. This device is a folded parallel plate transmission line; (b) voltage as a function of time at the bc gap of the module shown in (a).

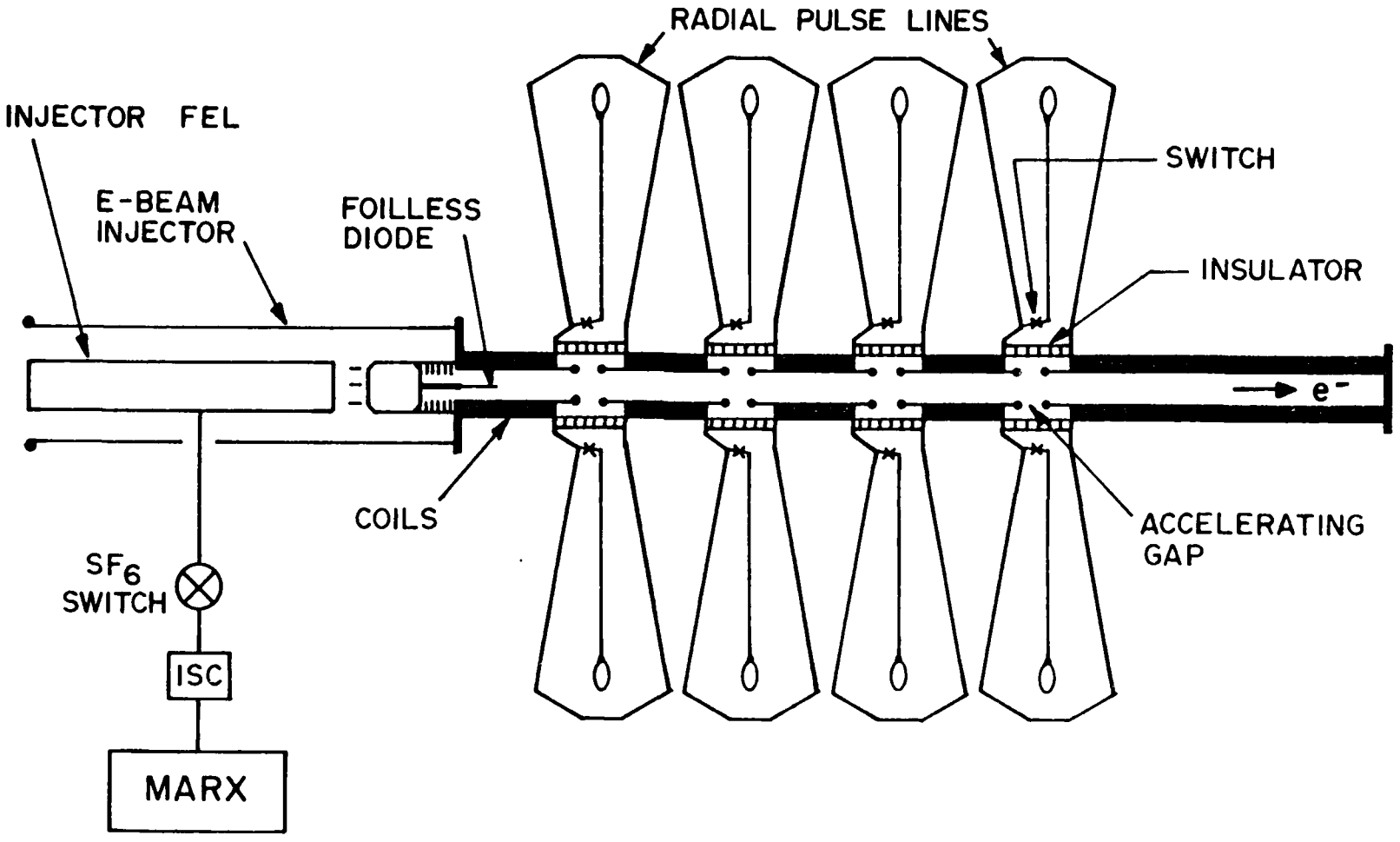

Fig. 4 Schematic of Radlac I. The four radial lines are filled with oil and are triggered with self-breaking spark gap switches.

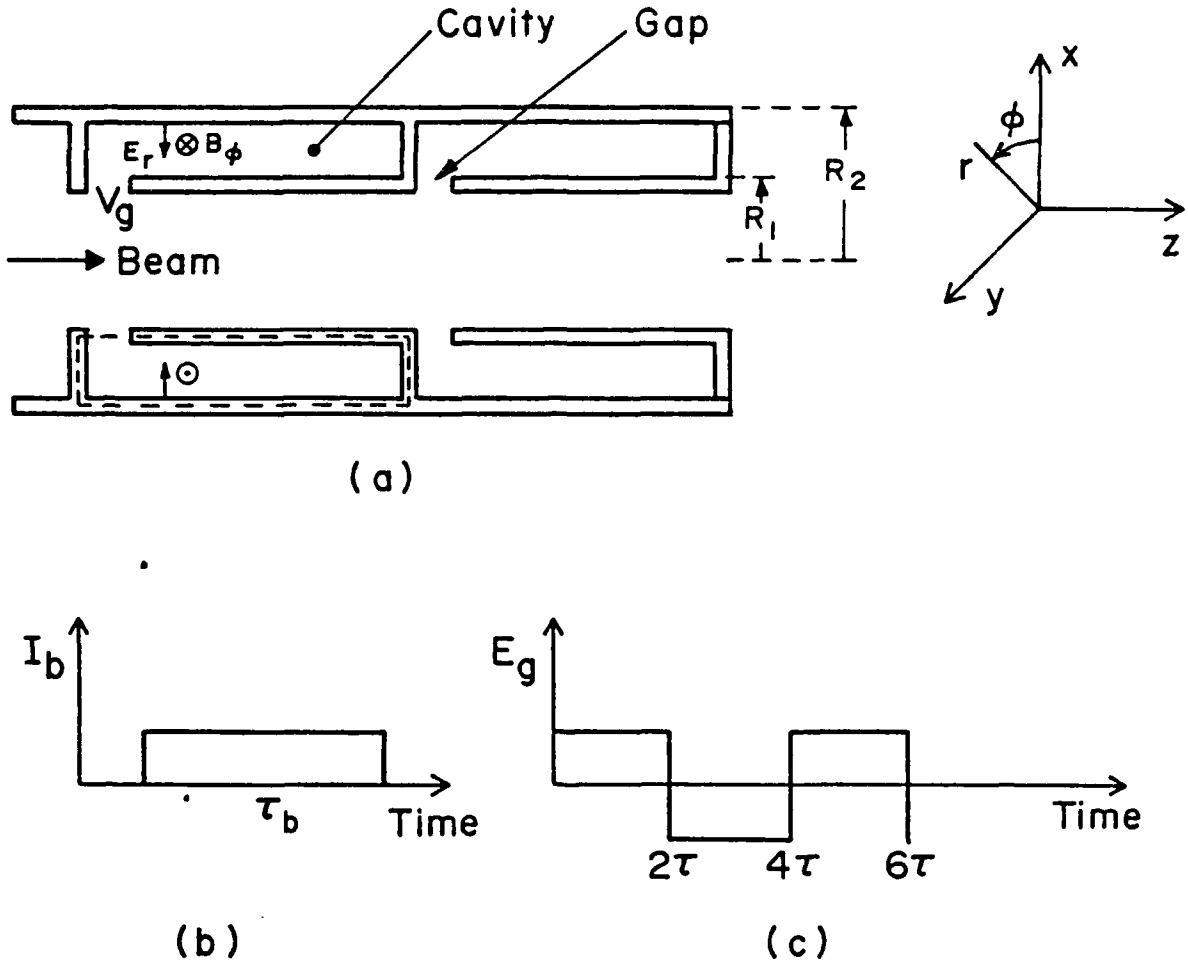

Fig. 5 Schematic of a two axial cavity auto-accelerator; (b) electron beam current as a function of time; (c) electric field at the gap as a function of time

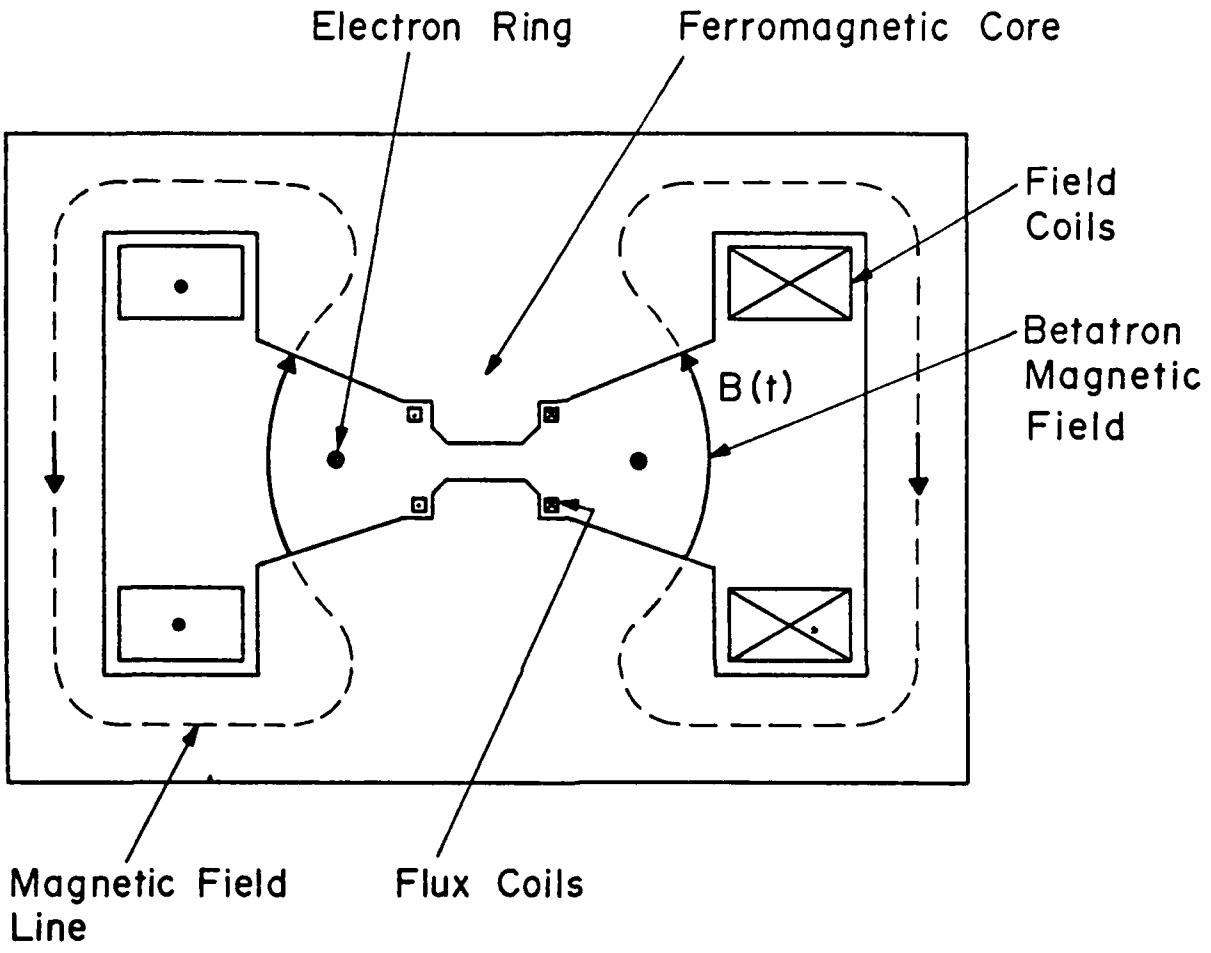

Fig. 6 Schematic of an "iron-core" conventional betatron.

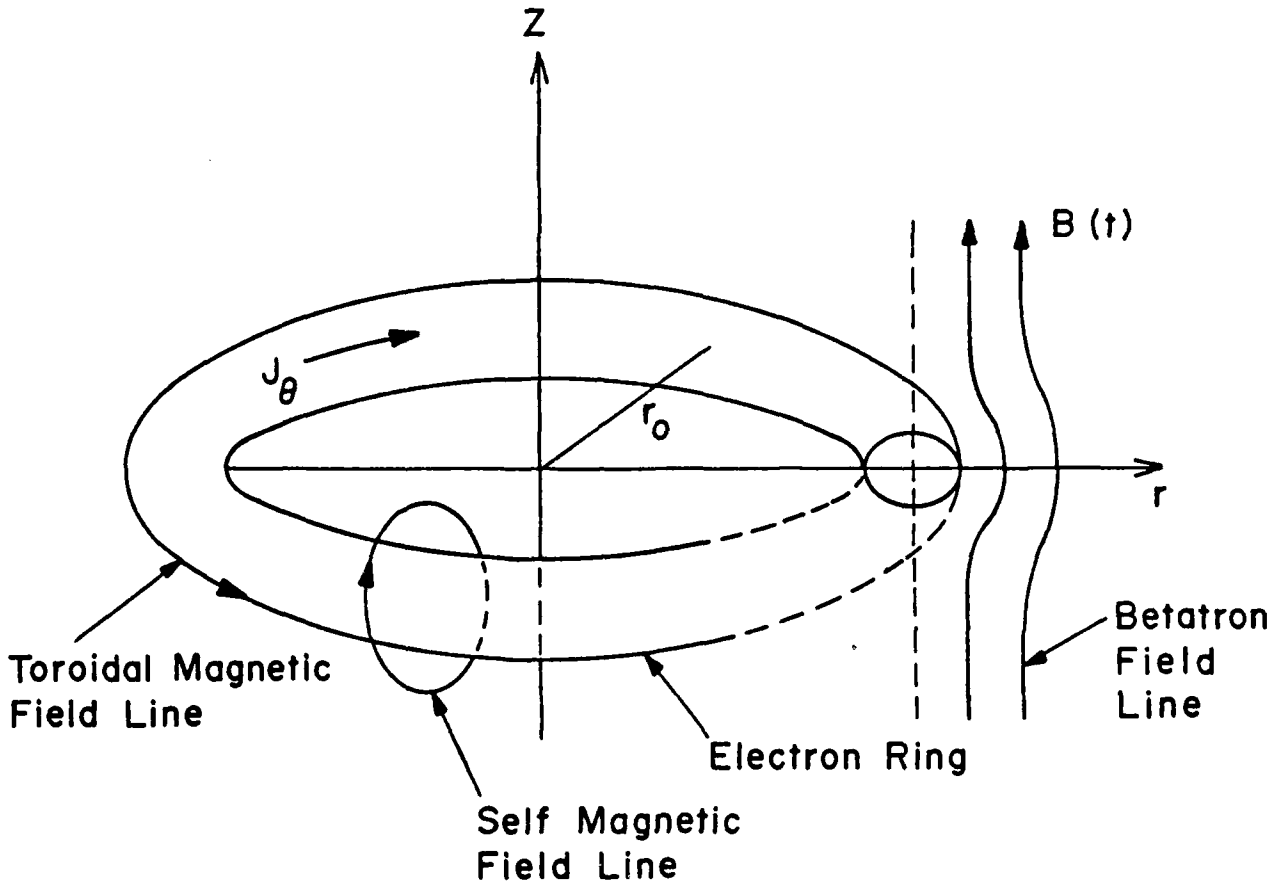

Fig. 7 Schematic of a modified betatron.

References

1. H. H. Fleischmann, Phys. Today, V. 28, #5, (May 1975). p. 34.
2. J. A. Nation, Particle Accelerators 10, 1 (1979).
3. J. Golden, C. A. Kapetanakos, J. A. Pasour and R. A. Mahaffey, Am. Scientist 69, 173 (1981).
4. P. Sprangle and T. Coffey, Phys. Today, V. 36, #12, (Dec 1983).
5. Physics Today, V. 36, #8, (August 1983), p. 17.
6. N. C. Christofilos, et al., Rev. Sci. Instrum. 35, 886 (1964).
7. J. E. Leiss, N. J. Norris and M. A. Wilson, Part. Acc. 10, 223 (1980).
8. D. Keefe, Part. Acc. 11, 187 (1981).
9. T. J. Fessenden, et al.; Proc. of the Int. Top. Conf. on High-Power Electron and Ion Beam Research and Technology; Palaiseau, France, June 29-July 3, 1981, p. 813. AD-A057 218 Vol I, AD A057 219 Vol. II, March 78, edition.
10. R. Briggs, Proc. 1981 Particle Accel. Conf.; to be published in IEEE Trans. Nucl. Sci. NS-28 (June 1981).
11. A. I. Pavlovskii, et al., Sov. Phys. Dokl. 25, 120 (1980).
12. K. R. Prestwich, et al., IEEE Trans. on Nucl. Sci. NS-30, 3155 (1983).
13. L. N. Kazanskii, A. V. Kisletsov and A. N. Lebedev, Atomic Energy 30, 27 (1971).
14. M. Friedman, Appl. Phys. Lett. 41, 419 (1982).
15. D. W. Kerst, Nature 157, 90 (1946).
16. A. I. Pavlovskii, et al., Sov. Phys. Tech. Phys. 22, 218 (1977).
17. C. A. Kapetanakos, S. J. Marsh and P. Sprangle, NRL Memo Report No. 5108, (1983), "Dynamics of a High Current Electron Ring in a Conventional Betatron Accelerator." (AD-A133 291).

18. A. G. Bonch-Osmolovskii, G. V. Dolbilow, I. N. Ivanov, E. A. Perelshtein, V. P. Sarantsev, O. I. Yarkovoy, JINR-Report P9-4135 Dubna (USSR) 1968.

19. P. Sprangle and C. A. Kapetanakos, J. Appl. Phys. 49, 1 (1978).

20. N. Rostoker, Comments on Plasma Physics, Vol. 6, p. 91 (1980).

21. C. A. Kapetanakos, P. Sprangle, D. P. Chernin, S. J. Marsh and I. Haber, NRL Memo Report 4905 (1981); also Phys. of Fluids (1983). (AD-A 119 869)

22. C. W. Roberson, A. Mondelli and D. Chernin, Phys. Rev. Lett. 50, 507 (1983).

23. P. Sprangle and D. Chernin, NRL Memo Report No. 5176 (1983). (AD-A133-337)

24. P. Sprangle and C. A. Kapetanakos, NRL Memo Report No. 4950 (1983). (ADA128 242)

25. P. Sprangle and J. Vomvoridis, NRL Memo Report No. 4688 (1981).

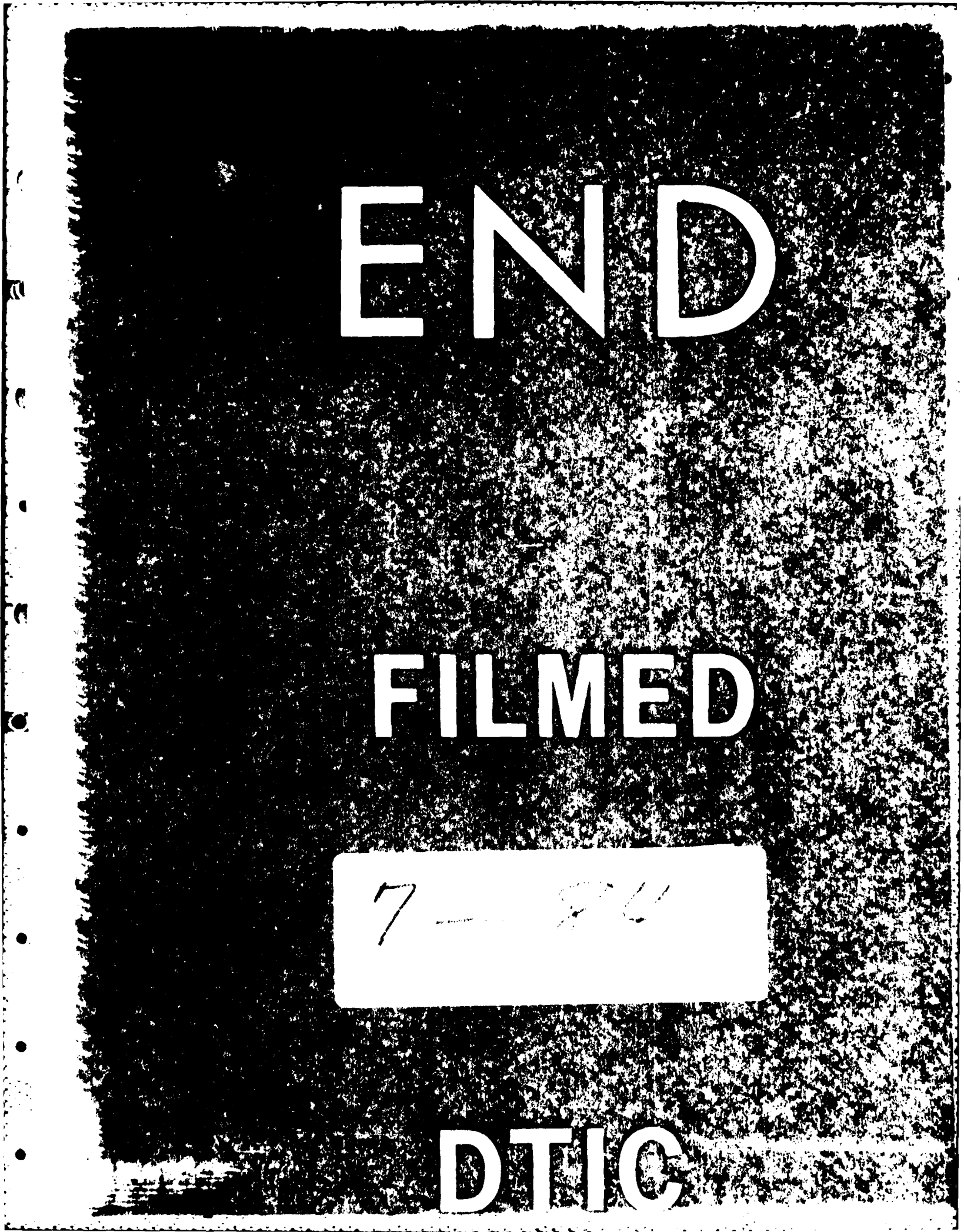
END
FILMED
7-84
DTIC